

## REPORT No. 634

# CALCULATION OF THE CHORDWISE LOAD DISTRIBUTION OVER AIRFOIL SECTIONS WITH PLAIN, SPLIT, OR SERIALLY HINGED TRAILING-EDGE FLAPS

By H. JULIAN ALLEN

### SUMMARY

*A method is presented for the rapid calculation of the incremental chordwise normal-force distribution over an airfoil section due to the deflection of a plain flap or tab, a split flap, or a serially hinged flap. This report is intended as a supplement to N. A. C. A. Report No. 631, wherein a method is presented for the calculation of the chordwise normal-force distribution over an airfoil without a flap or, as it may be considered, an airfoil with flap (or flaps) neutral.*

*The calculations are made possible through the correlation, by means of thin-airfoil theory, of numerous experimental normal-force distributions. The method enables the determination of the form and magnitude of the incremental normal-force distribution to be made for an airfoil-flap combination for which the section characteristics have been determined.*

*A method is included for the calculation of the flap normal-force and hinge-moment coefficients without necessitating a determination of the normal-force distribution.*

### INTRODUCTION

The general importance of airfoils equipped with trailing-edge flaps has promoted both experimental and theoretical determinations of the chordwise distribution of normal force over such surfaces in an effort to increase the structural efficiency of their design.

The theoretical investigations have been made under the assumption that the fluid viscosity is negligibly small. This assumption must be made, for the present at least, in order that the problem may be analytically handled. Unfortunately, as experiments have shown, viscosity clearly is not a negligible factor in this problem and, consequently, the theory is not able to predict adequately either the magnitude of the incremental normal force brought about by the deflection of the flaps or the nature of the chordwise distribution of this incremental normal force.

On the other hand, the large number of variables involved in the problem makes it too difficult to develop an adequate method, applicable in the general case, for the calculation of the incremental normal force and the incremental normal-force distribution from the experimental pressure-distribution measurements that have been made.

In this report a method is developed for the calculation of the incremental normal-force distribution due to the deflection of the flap based upon the results of experimental investigations; the theoretical relationships are used as a basis for the coordination of the experimental observations. Employment of experimentally determined airfoil section characteristics makes it possible, moreover, to obtain a distribution consistent in magnitude with that obtained by experiment. The method has been made applicable to an airfoil section equipped with a plain flap or tab, a split flap, or a serially hinged flap. This report is intended as a supplement to reference 1, wherein a method, similar in its details of development, is presented for the calculation of the chordwise normal-force distribution over an airfoil section without a flap or, as it may be considered, an airfoil section with flap (or flaps) neutral.

In order to facilitate the employment of this method, the report has been divided into two sections:

I. The Derivation of the Method.

II. The Application of the Method.

In the derivation, Glauert's theoretical chordwise lift distribution is discussed and the empirical alteration of the theory is treated. In addition, the development of the requisite equations for the determination of the magnitude of the distribution from force-test results is given. In the application, the general procedure to be followed in using this method either for airfoil sections with plain or split flaps or for airfoil sections with serially hinged flaps is given in concise form along with an illustrative example. The mathematical derivation of the theory is given in the appendix.

### I. THE DERIVATION OF THE METHOD

Glauert (references 2 and 3) has treated analytically the problem of the symmetrical airfoil with a plain flap, assuming the airfoil to be of infinitesimal thickness. The thin-airfoil theory is treated in the appendix of this paper. It is shown that the incremental lift distribution or, as it will be regarded, the incremental normal-force distribution due to the deflection of a flap may be considered, for convenience, to be composed of two component distributions: (a) the incre-

mental additional distribution  $P_{ab}$ , and (b) the incremental basic distribution  $P_{bb}$ . The incremental additional distribution is, in form, independent of the flap-chord ratio and does not contribute to the quarter-chord pitching moment, whereas the incremental basic distribution is, in form, dependent upon the flap-chord ratio and is responsible for the entire incremental quarter-chord pitching moment due to the deflection of the flap.

The theoretical additional distribution, as given by the thin-airfoil theory (appendix, equation (A-17)), is shown by the dotted curve in figure 1. Since the incre-

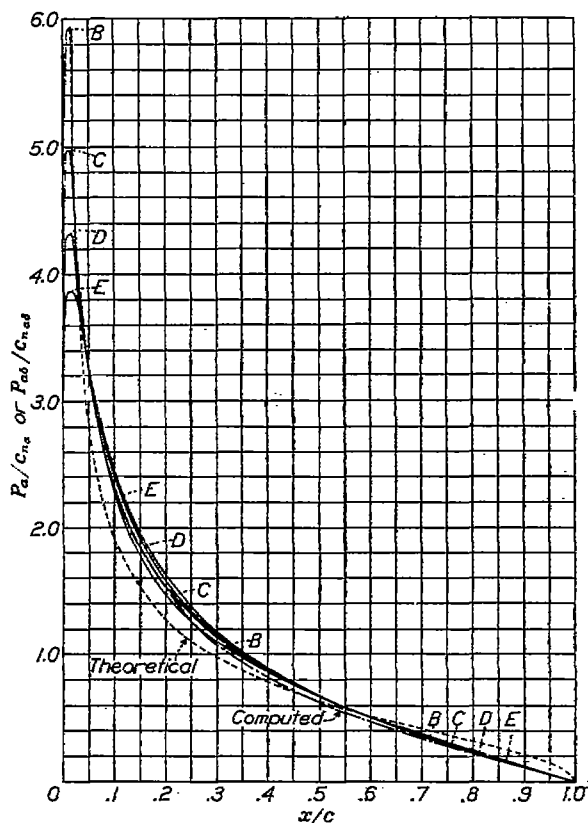


FIGURE 1.—Additional normal-force distributions.

mental additional distribution due to the deflection of the flap is identical in form with the additional distribution for the airfoil with flaps neutral, the experimentally determined additional distributions given in reference 1 will be used for this method. The four classes of additional distribution presented in reference 1 are given in table I and figure 1 (solid lines) of the present report. A key to the class of distribution to be employed for 22 airfoils is given in table II of the present report. (The letters A, B, C, D, and E in column "Classification PD" designate the class of distribution.) The remaining airfoil characteristics for these airfoils are given in table I of reference 1.

The shape of the theoretical incremental basic lift distribution (appendix, equation (A-19)) or, of what is considered to be its equivalent, the incremental basic

normal-force distribution is shown by the dotted lines of figures 2 to 6. Proceeding rearward from the leading edge of the airfoil, the pressure difference, which is zero at the leading edge, increases rapidly at first, then more slowly and, as the hinge is approached, it increases more and more rapidly until the pressure difference becomes unlimited at the hinge point, where the airfoil radius of curvature is zero. Rearward from the hinge, the pressure difference drops rapidly at first, then more slowly, and finally more rapidly again to zero pressure difference at the trailing edge. With a hinge radius of curvature other than zero, the basic pressure difference at the hinge becomes finite.

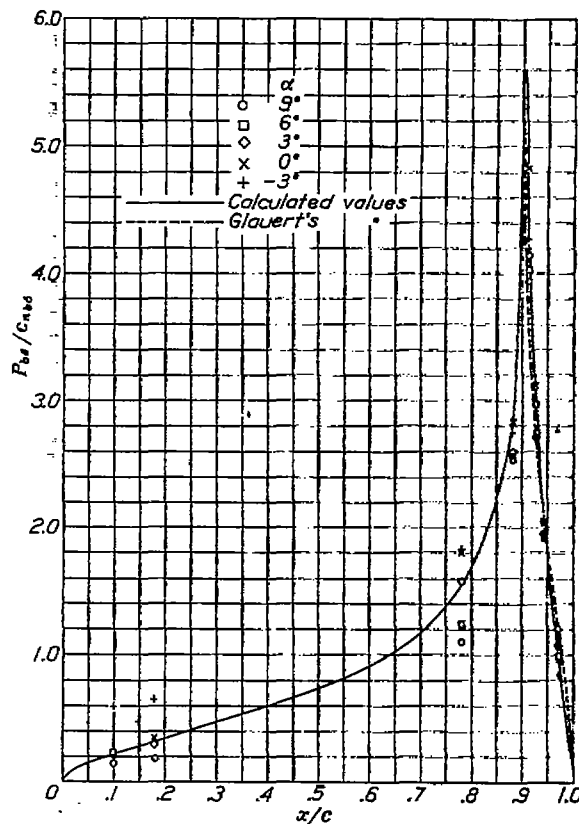


FIGURE 2.—Basic incremental normal-force distribution. R. A. F. 30 section; 0.10c plain flap at  $\delta=10^\circ$ .

Numerous comparisons between experimental (made with 0.10c, 0.20c, and 0.30c plain-flap airfoils with flap deflections ranging from  $10^\circ$  to  $60^\circ$ ) and theoretical incremental basic normal-force distributions ( $P_{bb}/c_{nbb}$ ) for plain-flap airfoils generally showed good agreement ahead of the hinge but poor agreement behind the hinge, particularly for large flap angles. This result is to be anticipated for ahead of the hinge favorable pressure gradients retard the growth of the boundary layer and, conversely, back of the hinge adverse gradients accelerate the growth of the boundary layer. An examination of these comparisons, however, disclosed that, for all three flap-chord ratios at any one given flap deflection, the ratio of the experimental basic normal

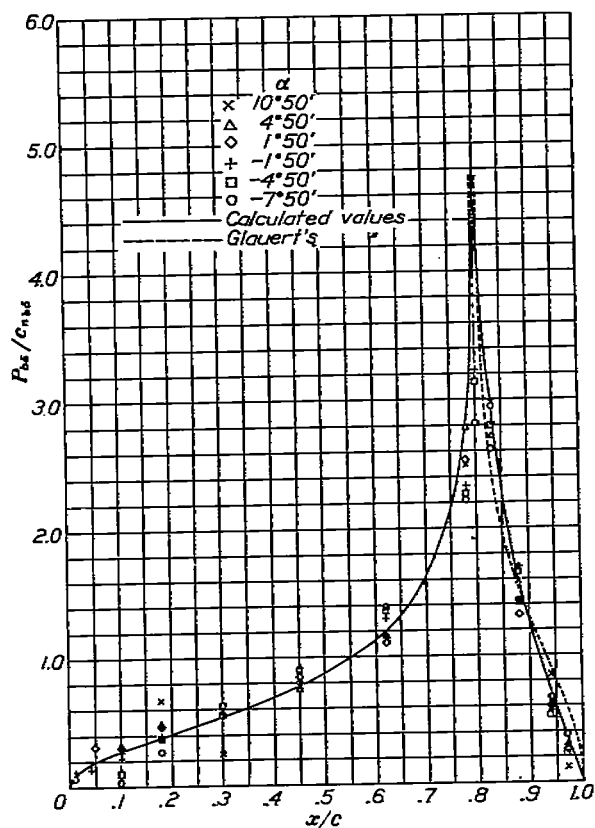


FIGURE 3.—Basic incremental normal-force distribution. R. A. F. 30 section; 0.20c plain flap at  $\delta=10^\circ$ .

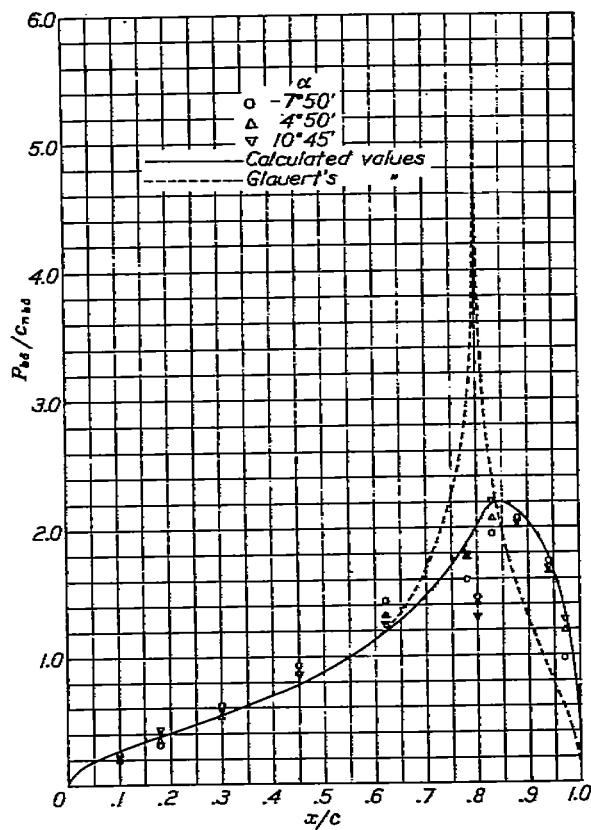


FIGURE 5.—Basic incremental normal-force distribution. R. A. F. 30 section; 0.20c plain flap at  $\delta=50^\circ$ .

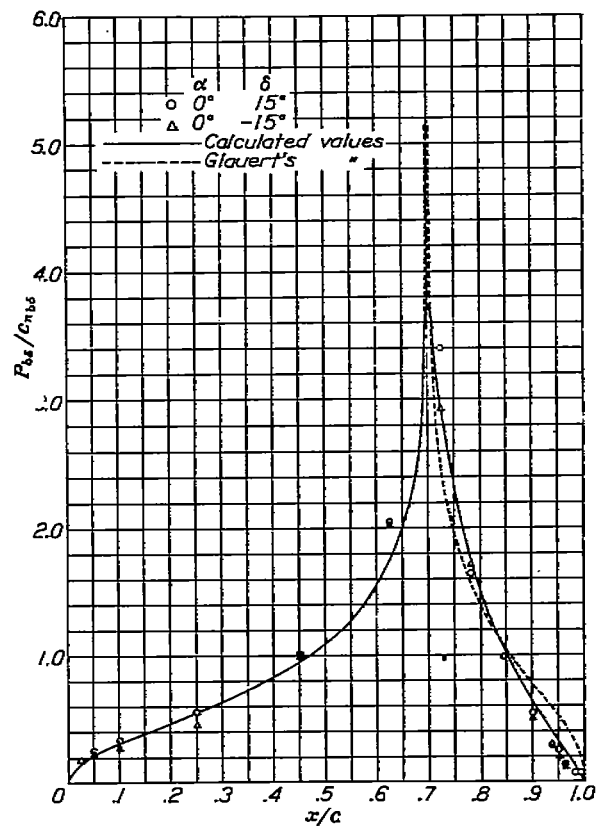


FIGURE 4.—Basic incremental normal-force distribution. Clark Y section; 0.20c plain flap at  $\delta=\pm 15^\circ$ .

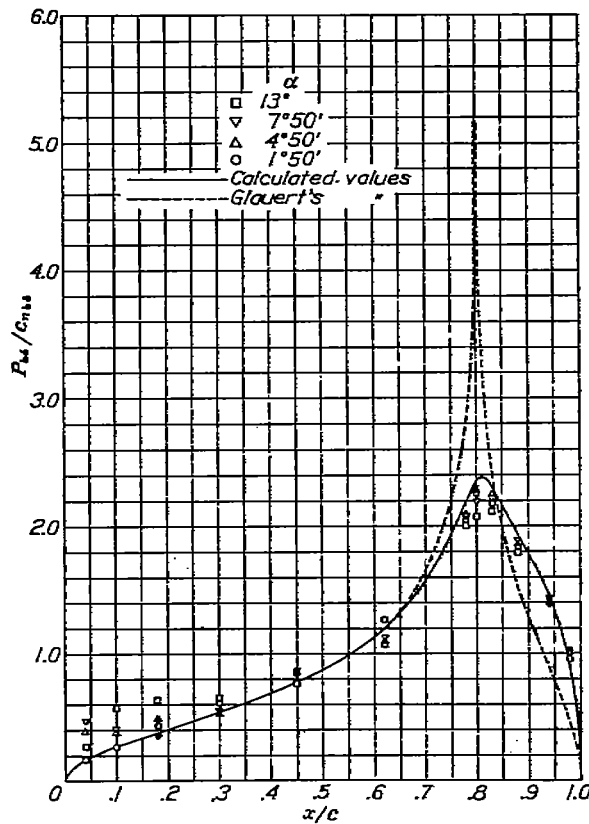


FIGURE 6.—Basic incremental normal-force distribution. R. A. F. 30 section; 0.20c plain flap at  $\delta=3^\circ$ .

force to the theoretical was practically constant for corresponding points along the airfoil. That is, if  $\beta$  is defined as

$$\beta = \frac{\left(\frac{P_{\delta\delta}}{c_{n_{\delta\delta}}}\right)_{exp.}}{\left(\frac{P_{\delta\delta}}{c_{n_{\delta\delta}}}\right)_{theor.}} \quad (1)$$

it has been found that values of  $\beta$  computed from experimental pressure-distribution measurements made over 0.10c, 0.20c, and 0.30c plain-flap airfoils with the same flap deflection (references 4 and 5), when plotted in the form of curves of  $\beta$  against both  $\frac{x/c}{1-E}$  (points ahead of the hinge) and  $\frac{1-(x/c)}{E}$  (points back of the hinge), lie very nearly on the same curve. In these expressions,  $E$  is the flap-chord ratio.

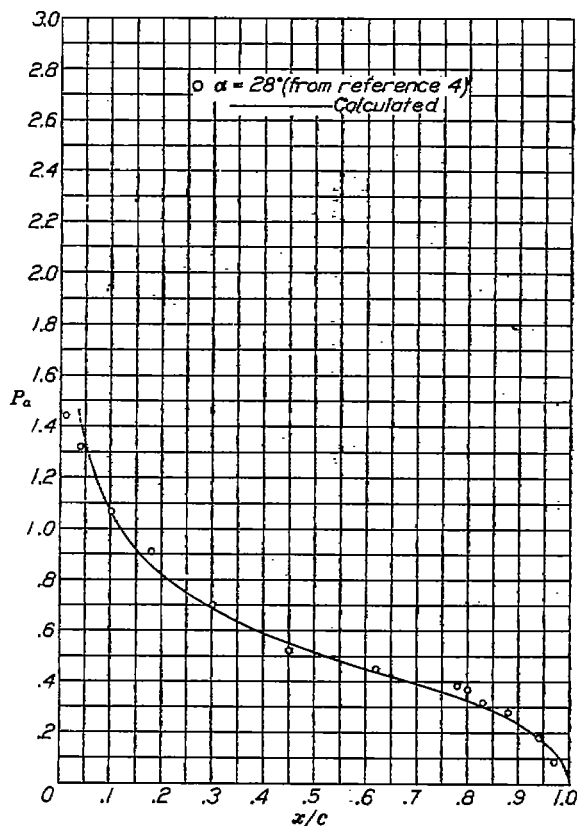


FIGURE 7.—Additional normal-force distribution for a stalled symmetrical airfoil. R. A. F. 30 section.

This result is used as a basis for extending the analysis to cases where no experimental data are available. Curves of the mean values of  $\beta$  for flap deflections of 10° to 60° were determined. It was found that, for flap deflections of 15° or less, a single  $\beta$  curve applied. At these small angles the departure between theory and experiment is slight, which shows that the boundary layer is still thin and the flow pattern is still reasonably like that predicted by theory. As the flap deflection is increased, the adverse pressure gradients back of the hinge are increased and separation finally takes place;

the incremental basic normal-force distribution then becomes markedly different from that predicted by theory. This abrupt change in the nature of the flow takes place at or near 20° flap deflection. The exact angle at which this stalling occurs is a function of a number of variables (angle of attack, Reynolds Number, surface irregularities, hinge leakage) and no single  $\beta$  curve can apply very near this flap angle.

Values of  $P_{\delta\delta}/c_{n_{\delta\delta}}$  have been computed from numerous pressure-distribution measurements (references 4 and 5) and are plotted in figures 2 to 6 along with the theoretical distributions and the computed distributions obtained by use of the computed curves of mean  $\beta$  values.

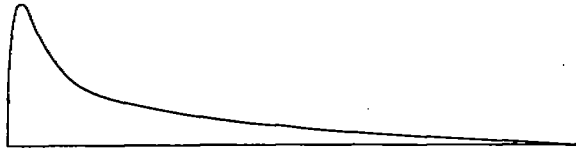
In table III (a) to (f), the computed distributions of  $P_{\delta\delta}/c_{n_{\delta\delta}}$  (equation (1)) are given for various flap-chord ratios and flap deflections.

The expansion of the experimental results, taken with plain flaps where the flap-chord ratio never exceeded 0.30, to the much higher values given in table III is justified as follows. When the flap-chord ratio is 1.0 for a symmetrical airfoil, the incremental normal-force distribution becomes the incremental additional normal-force distribution and, when corrected by the mean  $\beta$  values, the incremental additional distribution should be expected to agree with the experimentally determined additional distribution if the  $\beta$  values are truly independent of the flap-chord ratio. In figure 1, the computed distribution obtained by use of the  $\beta$  values for the unstalled flow (i. e.,  $\delta=5^\circ$ ,  $10^\circ$ , and  $15^\circ$ ) is shown along with the additional distributions of reference 1. In figure 7, the computed and experimental distributions for a stalled symmetrical airfoil ( $\alpha=\delta=28^\circ$ ) are shown. From the close agreement between the experimental and the computed distributions shown in figures 1 to 4 for the unstalled flap and in figures 5 to 7 for the stalled airfoil, it is concluded that, for design purposes, the  $\beta$  values may be considered independent of the flap-chord ratio.

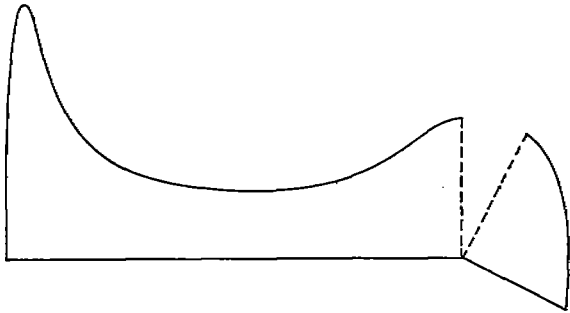
The method of correlating experimental pressure distributions for airfoils with plain flaps may be employed for airfoils with split flaps. Consider the airfoils with split flaps to be analogous to the airfoils with plain flaps, the boundary-layer displacement thickness at any point back of the hinge for the airfoils with split flaps being as great as the distance from the lower surface of the flap to the upper surface of the undeflected portion of the airfoil back of the hinge. Analysis of the problem in this manner permits the values of  $\beta$  to be determined from experimental data, provided that some assumption is made regarding the lift distribution on the undeflected portion of the airfoil back of the hinge. Assume that over this portion at all points back of the hinge the pressure differences are negligibly small compared with the corresponding pressure differences over the split flap itself. This assumption is consistent with the analogy (pressures are propagated undiminished

through a boundary layer) and is supported fairly well by experiment (references 6 and 7), particularly for positive angles of attack and the larger flap deflections.

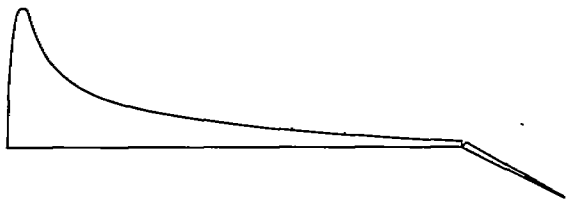
Values of  $\beta$  were obtained for split flaps using the incremental pressure distributions of reference 6. It was found that, for flap deflections of  $40^\circ$  or more, the



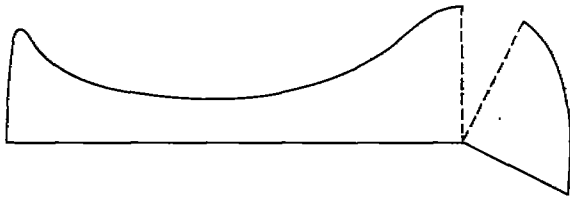
(a) Normal-force distribution for airfoil with flap neutral.



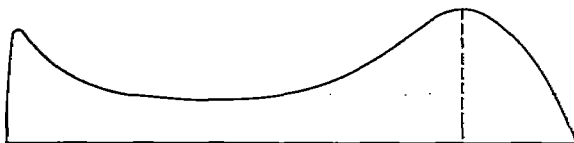
(b) Normal-force distribution for airfoil with flap deflected.



(c) Distribution shown in (a) plotted normal to flap-deflected chord.



(d) Increment normal-force distribution due to deflection of flap.



(e) Distribution shown in (d) plotted normal to flap-neutral chord.

FIGURE 8.—Normal-force distribution and incremental normal-force distribution for flaps neutral and deflected.

$\beta$  values for plain- and split-flap airfoils were the same. In table III (d) to (h), the computed distributions of  $P_{ds}/c_{n_{ds}}$  are given for various flap-chord ratios and flap

deflections. Again the assumption is made that a single  $\beta$  curve applies for all flap-chord ratios for any given flap deflection.

The development of the requisite equations to determine the magnitude of the incremental additional and incremental basic distribution from wind-tunnel force tests will now be considered. From force tests of the airfoil with flap neutral,  $c_{m_1}$  (quarter-chord pitching-moment coefficient) and  $c_{n_1}$  (normal-force coefficient) corresponding to the normal-force distribution shown in figure 8 (a) are obtained. Again, from force tests of the airfoil at the same attitude with the flap deflected,  $c_{m_2}$  and  $c_{n_2}$  corresponding to the normal-force distribution shown in figure 8 (b) are obtained.

Let

$$\left. \begin{aligned} \Delta c_m &= c_{m_2} - c_{m_1}' \\ \Delta c_n &= c_{n_2} - c_{n_1}' \end{aligned} \right\} \quad (2)$$

where  $c_{m_1}'$  and  $c_{n_1}'$  are the pitching-moment and normal-force coefficients corresponding to the normal-force distribution for the airfoil with flap neutral when plotted normal to the chord of the airfoil with flap deflected, as shown in figure 8 (c). Then  $\Delta c_m$  and  $\Delta c_n$  are the pitching-moment and normal-force coefficients of the incremental normal-force distribution when the incremental distribution is plotted normal to the chord of airfoil with flap deflected, as shown in figure 8 (d).

For the commonly used airfoils, the approximation

$$\left. \begin{aligned} c_{n_1} &= c_{n_1}' \\ c_{m_1} &= c_{m_1}' \end{aligned} \right\} \quad (3)$$

is sufficiently exact except in the rare case when the flap-chord ratio  $E$  and the flap deflection  $\delta$  are simultaneously large. (See figs. 8 (a) and (c).)

Let  $\Delta c_m'$  and  $\Delta c_n'$  be the pitching-moment and the normal-force coefficients of the incremental normal-force distribution plotted normal to the flap-neutral chord, as shown in figure 8 (e). Since the incremental basic normal-force distribution is responsible for the entire quarter-chord pitching moment, then, if  $G$  is the moment arm in terms of the chord of the basic normal force about the quarter-chord point,

$$\Delta c_m' = G c_{n_{ds}}$$

$$\Delta c_n' = c_{n_{ds}} + c_{n_{ds}}$$

or

$$\left. \begin{aligned} c_{n_{ds}} &= \frac{\Delta c_m'}{G} \\ c_{n_{ds}} &= \Delta c_n' - \frac{\Delta c_m'}{G} \end{aligned} \right\} \quad (4)$$

The value of  $G$  is a function of  $E$  and  $\delta$ . Values of  $G$  are given in table IV.

The correlation between the fictitious values of  $\Delta c_m'$  and  $\Delta c_n'$  and the measured values of  $\Delta c_m$  and  $\Delta c_n$  must be established in order to determine  $c_{n_{ds}}$  and

$c_{n_{\delta}}$  from force tests. Let the incremental flap normal-force coefficient for unit span be given by

$$c_{n_{\delta}} = \frac{n_{\delta}}{qEc} \quad (5)$$

where  $n_{\delta}$  is the incremental flap normal force per unit span and  $q$  is the dynamic pressure in the air stream. Then

$$\left. \begin{aligned} \Delta c_n' &= \Delta c_n + Ec_{n_{\delta}}(1 - \cos \delta) \\ \Delta c_m' &= \Delta c_m - Ec_{n_{\delta}}(1 - \cos \delta) \left( \frac{3}{4} - E \right) \end{aligned} \right\} \quad (6)$$

The incremental flap normal force may be considered as a combination of two components due to the incremental additional and the incremental basic normal-force distributions. Let  $\gamma_{\delta}$  and  $\gamma_{b\delta}$  be the ratio of the flap normal force to the airfoil normal force for the incremental additional and the incremental basic normal forces, respectively; then

$$c_{n_{\delta}} = \gamma_{\delta} c_{n_{\delta}} + \gamma_{b\delta} c_{n_{b\delta}} \quad (7)$$

or

$$c_{n_{\delta}} = \gamma_{\delta} \left( \Delta c_n' - \frac{\Delta c_m'}{G} \right) + \gamma_{b\delta} \frac{\Delta c_m'}{G} \quad (8)$$

The contribution of the additional normal-force distribution is small compared with the basic contribution so that, for the purpose of determining  $\Delta c_m'$  and  $\Delta c_n'$ , the following approximation may be employed:

$$c_{n_{\delta}} = \gamma_{b\delta} \frac{\Delta c_m'}{G}$$

and equations (6) become

$$\begin{aligned} \Delta c_n' &= \Delta c_n + E\gamma_{b\delta} \frac{\Delta c_m'}{G} (1 - \cos \delta) \\ \Delta c_m' &= \Delta c_m - E\gamma_{b\delta} \frac{\Delta c_m'}{G} (1 - \cos \delta) \left( \frac{3}{4} - E \right) \end{aligned}$$

so that

$$\left. \begin{aligned} \Delta c_m' &= \tau_m \Delta c_m \\ \Delta c_n' &= \Delta c_n + \tau_n \Delta c_m \end{aligned} \right\} \quad (9)$$

where

$$\begin{aligned} \tau_n &= \frac{E(1 - \cos \delta) \frac{\gamma_{b\delta}}{G}}{1 + \left[ E(1 - \cos \delta) \left( \frac{3}{4} - E \right) \frac{\gamma_{b\delta}}{G} \right]} \\ \tau_m &= \frac{1}{1 + \left[ E(1 - \cos \delta) \left( \frac{3}{4} - E \right) \frac{\gamma_{b\delta}}{G} \right]} \end{aligned}$$

The values of  $\tau_n$  and  $\tau_m$  have been determined and are given in tables V and VI.

Then, given  $c_{n_2}$ ,  $c_{n_1}$ ,  $c_{m_2}$ , and  $c_{m_1}$  ( $c_i$  may be considered as  $c_n$ ;  $c_m$  may be calculated if  $c_{m_{a.c.}}$ , the pitching-moment coefficient about the aerodynamic center, and  $x_{a.c.}/c$ , the chordwise distance of the aerodynamic center from the quarter-chord point of the section in terms of the chord, are given instead of  $c_m$ )

$$\left. \begin{aligned} \Delta c_m &= c_{m_2} - c_{m_1} \\ \Delta c_n &= c_{n_2} - c_{n_1} \end{aligned} \right\} \quad (10)$$

and using the values of  $\tau_n$  and  $\tau_m$  from tables V and VI depending on the type of flap, then (equation (9))

$$\begin{aligned} \Delta c_m' &= \tau_m \Delta c_m \\ \Delta c_n' &= \Delta c_n + \tau_n \Delta c_m \end{aligned}$$

The incremental basic and additional normal-force coefficients may be obtained from equations (4), which are

$$\begin{aligned} c_{n_{b\delta}} &= \frac{\Delta c_m'}{G} \\ c_{n_{a\delta}} &= \Delta c_n' - \frac{\Delta c_m'}{G} \end{aligned}$$

When the appropriate values of the incremental basic normal-force distribution,  $P_{b\delta}/c_{n_{b\delta}}$ , from table III are used, then

$$P_{b\delta} = \left( \frac{P_{b\delta}}{c_{n_{b\delta}}} \right) c_{n_{b\delta}} \quad (11)$$

By the use of the proper class of incremental additional normal-force distribution,  $P_{a\delta}/c_{n_{a\delta}}$ , from table I

$$P_{a\delta} = \left( \frac{P_{a\delta}}{c_{n_{a\delta}}} \right) c_{n_{a\delta}} \quad (12)$$

The incremental basic and additional distributions may be added to give the entire incremental normal-force distribution,

$$P_{\delta} = P_{a\delta} + P_{b\delta} \quad (13)$$

and this incremental normal-force distribution may be added to the distribution for the airfoil section with undeflected flap,  $P_1$  (which distribution may be obtained by the method of reference 1), to give the normal-force distribution for the airfoil with the deflected flap

$$P_2 = P_1 + P_{\delta} \quad (14)$$

The incremental flap normal-force coefficient is given by equation (7) and the corresponding flap hinge-moment coefficient can be written by analogy.

$$\left. \begin{aligned} c_{h_{\delta}} &= \frac{n_{\delta}}{qEc} = \gamma_{\delta} c_{h_{\delta}} + \gamma_{b\delta} c_{h_{b\delta}} \\ c_{h_{\delta}} &= \frac{h_{\delta}}{qE^2 c^2} = \eta_{\delta} c_{h_{\delta}} + \eta_{b\delta} c_{h_{b\delta}} \end{aligned} \right\} \quad (15)$$

Values of  $\gamma_{\delta}$  and  $\eta_{\delta}$  are given in tables VII and VIII. As the incremental additional and additional distributions are identical in form

$$\begin{aligned} \gamma_{a\delta} &= \gamma_a \\ \eta_{a\delta} &= \eta_a \end{aligned}$$

Values of  $\gamma_a$  and  $\eta_a$  are given in tables IX and X, respectively.

The flap normal-force and hinge-moment coefficients for the airfoil with flap neutral may be determined by considering the contributions of each of the component distributions that make up the flap-neutral normal-force distribution. In reference 1 the flap-neutral normal-force distribution is considered to be composed of four component distributions: (a) the moment basic (class 1), (b) the camber basic (class 0, 1, or 2), (c) the aerodynamic center, and (d) the additional (classes A, B, C, D, and E). The class of each distribution to be employed for a number of airfoils is given in table II (or tables I and II of reference 8) in the column "Classification PD." The letter (A, B, C, D, or E) designates the class of the additional distribution; the first number (1) designates the class of the moment basic distribution; the second number (0, 1, or 2) designates the class of the camber basic distribution.

The moment basic normal-force coefficient may be obtained from

$$c_{n_{bm}} = -6.30 c_{m_{a.c.1}} \text{ for class 1} \quad (16)$$

The camber basic normal-force coefficient may be obtained from

$$\left. \begin{aligned} c_{n_{bc}} &= 0 && \text{for class 0} \\ c_{n_{bc}} &= 9.70 \frac{z_c}{c} && \text{for class 1} \\ c_{n_{bc}} &= 18.75 \frac{z_c}{c} && \text{for class 2} \end{aligned} \right\} \quad (17)$$

where  $z_c/c$  is the camber in terms of the chord. Values of  $z_c/c$  are given for a small number of airfoils in table II and for a large number of airfoils in tables I and II of reference 8. The additional normal-force coefficient may be obtained from

$$c_{n_a} = c_{n_1} - c_{n_{bc}} - c_{n_{bm}} \quad (18)$$

The aerodynamic-center distribution coefficient is given by

$$c_{a.c.} = \frac{x_{a.c.}}{c} c_{n_a} \quad (19)$$

Values of  $x_{a.c.}/c$  are given for a small number of airfoils in table II (column 3) and for a large number in tables I and II of reference 8.

Finally, the flap normal-force coefficient is given by

$$c_{n_{f1}} = \gamma_a c_{n_a} + \gamma_{bc} c_{n_{bc}} + \gamma_{bm} c_{n_{bm}} + \gamma_{a.c.} c_{a.c.} \quad (20)$$

and the flap hinge-moment coefficient is given by

$$c_{h_{f1}} = \eta_a c_{n_a} + \eta_{bc} c_{n_{bc}} + \eta_{bm} c_{n_{bm}} + \eta_{a.c.} c_{a.c.} \quad (21)$$

The various  $\gamma$  and  $\eta$  values are given in tables IX and X.

The flap normal-force and hinge-moment coefficients for the airfoil section with flap deflected are

$$\left. \begin{aligned} c_{n_{f2}} &= c_{n_{f1}} + c_{n_{f\delta}} \\ c_{h_{f2}} &= c_{h_{f1}} + c_{h_{f\delta}} \end{aligned} \right\} \quad (22)$$

This method for the determination of incremental chordwise normal-force distribution for airfoils with flaps was developed for airfoils of normal profile and camber, and therefore it cannot be presupposed that this method might be applied to airfoil sections of abnormal form.

The values of  $P_{\delta\delta}/c_{n_{\delta\delta}}$  for airfoils with both plain and split flaps were determined from tests of airfoils having very small gaps between the wing and the leading edge of the flap. It has been found (reference 9) that any gap between the wing and the leading edge of a plain flap has a detrimental effect upon the aerodynamic characteristics. It is probable that this gap effect will also be true for split-flap airfoils. In the absence of evidence to the contrary, the method presented cannot be considered applicable to plain-flap or split-flap airfoils with large gaps.

The flap hinges of all plain-flap airfoils, from the tests of which the  $P_{\delta\delta}/c_{n_{\delta\delta}}$  values for the plain flap were determined, were midway between the upper and lower surfaces of the airfoils; that is, the radius of curvature of the upper surface above the hinge for each airfoil was half the depth of the airfoil at the hinge. Tests have been conducted to determine the effect of changing the radius of curvature at this point from zero to the full depth of the airfoil at the hinge. (The results of these tests have not been published.) The airfoil employed in the test was equipped with a 0.60c plain flap deflected 12° and with a 0.20c plain flap deflected 15°; the effect of changing the radius of curvature at the 0.60c-flap hinge alone was determined. The results of these tests show only a negligible change in the aerodynamic characteristics (and presumably in the normal-force distribution) with a change in the radius of curvature. Because of the limited nature of the tests, these results cannot be considered conclusive for plain-flap airfoils in general, and the method presented must be considered strictly applicable to plain-flap airfoils with upper-surface curvatures not less than half the airfoil depth at the hinge.

The  $P_{\delta\delta}/c_{n_{\delta\delta}}$  values for plain-flap airfoils were determined from airfoil tests made at an effective Reynolds Number of about 1,000,000. Comparison of these tests with tests made at an effective Reynolds Number of about 17,000,000 indicates that the effect of scale is unimportant although, it may be mentioned, in the critical region of flap deflections (i. e., for  $\delta$  near 20°) there is a tendency at higher scales to maintain the unstalled incremental basic distribution (i. e., the  $\delta=5^\circ$ , 10°, and 15° type of distribution) up to slightly greater flap deflections. Pressure-distribution measurements on split-flap airfoils made at effective Reynolds Numbers of 1,700,000 and 3,200,000 showed apparently no effect from this small change of scale.

It is difficult to make any general statement regarding the accuracy of this method for the determination of the

incremental chordwise normal-force distribution. The dispersion of experimental pressure-measurement results shown in figures 2 to 6 may be considered typical.

## II. THE APPLICATION OF THE METHOD

### THE GENERAL PROCEDURE FOR AN AIRFOIL WITH A PLAIN OR A SPLIT FLAP

In order to determine at a given lift coefficient the incremental normal-force distribution over a given airfoil section due to the deflection of a plain or a split flap, it is necessary to have the following experimentally determined characteristics for the airfoil section:

(a) With flap deflected:

$c_{l_2}$ , the section lift coefficient (given).

$c_{m_{a.c.2}}$ , the section pitching-moment coefficient about the aerodynamic center.

$\left(\frac{x_{a.c.}}{c}\right)_2$ , the chordwise coordinate of the aerodynamic-center position in terms of the chord.

(b) With flap neutral (with the airfoil section at the same angle of attack):

$c_{l_1}$ , the section lift coefficient.

$c_{m_{a.c.1}}$ , the section pitching-moment coefficient about the aerodynamic center.

$\left(\frac{x_{a.c.}}{c}\right)_1$ , the chordwise coordinate of the aerodynamic-center position in terms of the chord.

(c) The class of additional normal-force distribution to be employed.

For illustrative purposes, given: an N. A. C. A. 23012 airfoil section with a 0.20c split flap ( $E=0.20$ ) set at  $45^\circ$  ( $\delta=45^\circ$ ). To determine: the incremental normal-force distribution for this airfoil, when, with the flap deflected, the lift coefficient  $c_{l_2}$  is 1.40. From reference 10, when

$$c_{l_2}=1.40$$

then

$$c_{m_{a.c.2}}=-0.229$$

$$\left(\frac{x_{a.c.}}{c}\right)_2=0.012$$

$$\alpha=2.0^\circ$$

For the airfoil with flap retracted, when  $\alpha=2.0^\circ$ , from reference 11,

$$c_{l_1}=0.34$$

$$c_{m_{a.c.1}}=-0.005$$

and from table II of the present report

$$\left(\frac{x_{a.c.}}{c}\right)_1=0.012$$

and the C class of additional distribution is to be employed.

The quarter-chord pitching-moment coefficient is obtained from

$$c_m=c_{m_{a.c.}}+c_l\left(\frac{x_{a.c.}}{c}\right)$$

and the approximation is made

$$c_n=c_l$$

so that, for the example cited,

$$c_{m_2}=-0.229+1.40(0.012)=-0.212$$

$$c_{n_2}=1.40$$

and

$$c_{m_1}=-0.005+0.34(0.012)=-0.001$$

$$c_{n_1}=0.34$$

The quarter-chord pitching-moment and normal-force coefficients for the incremental normal-force distribution considered normal to the airfoil chord with flap deflected are given by

$$\left. \begin{aligned} \Delta c_m &= c_{m_2} - c_{m_1} \\ \Delta c_n &= c_{n_2} - c_{n_1} \end{aligned} \right\} \quad (10)$$

(equations are numbered as in part I of the report) so that, for the example cited,

$$\Delta c_m = -0.212 + 0.001 = -0.211$$

$$\Delta c_n = 1.40 - 0.34 = 1.06$$

The pitching-moment and normal-force coefficients for the incremental normal-force distribution, considered normal to the airfoil chord with flap neutral, are given by

$$\left. \begin{aligned} \Delta c_m' &= \tau_m \Delta c_m \\ \Delta c_n' &= \Delta c_n + \tau_n \Delta c_m \end{aligned} \right\} \quad (9)$$

Values of  $\tau_n$  and  $\tau_m$  are given in tables V and VI. For the example cited, by interpolation from the tables,

$$\tau_m = 1.16$$

$$\tau_n = -0.30$$

so that

$$\Delta c_m' = 1.16 (-0.211) = -0.245$$

$$\Delta c_n' = 1.06 + (-0.30) (-0.211) = 1.12$$

The incremental normal-force distribution is considered to be composed of two component distributions: (a) the incremental additional distribution, and (b) the incremental basic distribution. The magnitude of the incremental basic normal-force coefficient is given by

$$c_{n_{bs}} = \frac{\Delta c_m'}{G} \quad (4)$$

Values of  $G$  are given in table IV for airfoils with plain and split flaps.

For the example cited by interpolation from the table

$$G = -0.412$$

and so

$$c_{n_{bs}} = \frac{-0.245}{-0.412} = 0.60$$

The incremental additional normal force is obtained from

$$c_{n_{as}} = \Delta c_n' - c_{n_{bs}} \quad (4)$$



For the example cited

$$c_{n_{as}} = 1.12 - 0.60 = 0.52$$

The incremental additional distribution may then be obtained from

$$P_{as} = \left( \frac{P_{as}}{c_{n_{as}}} \right) c_{n_{as}} \quad (12)$$

Values of  $P_{as}/c_{n_{as}}$  at a number of stations along the chord are given for the various classes of distributions in table I and figure 1. The quantity  $P_{as}$  is the pressure difference in terms of  $q$ , the stream dynamic pressure.

For the example cited

$$P_{as} = \left( \frac{P_{as}}{c_{n_{as}}} \right) 0.52$$

so that for the class C distribution (table I) the values of  $P_{as}$  in the following table are obtained.

COMPUTATION OF INCREMENTAL ADDITIONAL DISTRIBUTION

$x/c$	$P_{as}/c_{n_{as}}$	$P_{as}$
0	0	0
.0125	4.98	2.59
.025	4.23	2.20
.050	3.22	1.67
.075	2.68	1.39
.100	2.32	1.21
.150	1.85	.96
.200	1.54	.80
.300	1.14	.59
.400	.87	.45
.500	.68	.35
.600	.51	.27
.700	.37	.20
.800	.24	.13
.900	.12	.06
.950	.06	.03
1.000	0	0

The incremental basic distribution is found from

$$P_{bs} = \left( \frac{P_{bs}}{c_{n_{bs}}} \right) c_{n_{bs}} \quad (11)$$

Values of  $P_{bs}/c_{n_{bs}}$  at a number of stations along the chord are given in table III for plain and split flaps.

For the example cited,

$$P_{bs} = \left( \frac{P_{bs}}{c_{n_{bs}}} \right) 0.60$$

Values of  $P_{bs}/c_{n_{bs}}$  are obtained by interpolation from table III and computed values of  $P_{bs}$  are given in the following table. Again,  $P_{bs}$  is the pressure difference in terms of  $q$ .

COMPUTATION OF INCREMENTAL BASIC DISTRIBUTION

$x/c$ 1-E	$x/c$	$P_{bs}/c_{n_{bs}}$	$P_{bs}$	$1-x/c$ E	$x/c$	$P_{bs}/c_{n_{bs}}$	$P_{bs}$
0	0	0	0	1.00	0.80	2.06	1.23
.05	.04	.16	.10	.90	.82	2.19	1.31
.10	.08	.24	.14	.80	.84	2.21	1.32
.20	.16	.35	.21	.70	.86	2.18	1.31
.30	.24	.46	.28	.60	.88	2.12	1.27
.40	.32	.57	.34	.50	.90	2.02	1.21
.50	.40	.69	.41	.40	.92	1.89	1.13
.60	.48	.83	.50	.30	.94	1.70	1.02
.70	.56	1.02	.61	.20	.96	1.47	.88
.80	.64	1.26	.75	.10	.98	1.10	.66
.90	.72	1.59	.95	.05	.99	.82	.49
1.00	.80	2.06	1.23	0	1.00	0	0

Finally the incremental normal-force distribution is found by addition:

$$P_s = P_{as} + P_{bs} \quad (13)$$

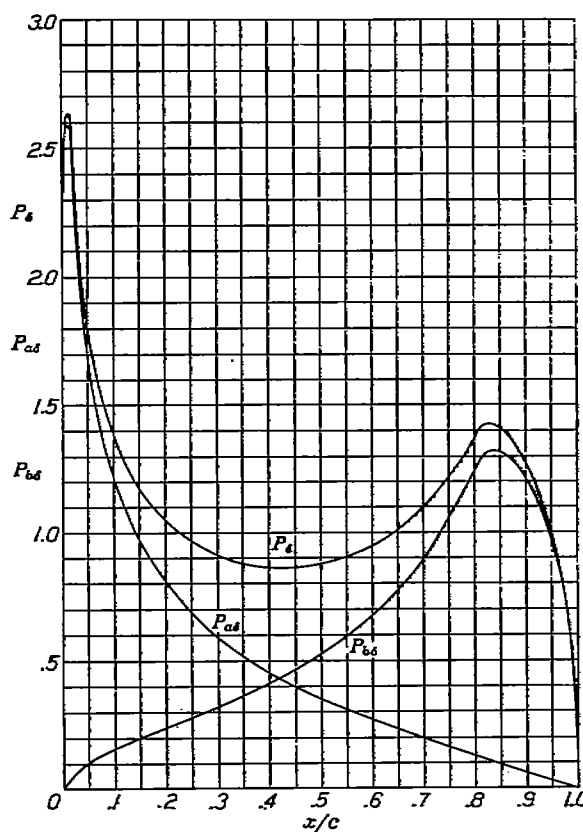


FIGURE 9.—Calculated incremental normal-force distribution. N. A. C. A. 23012 airfoil section at  $\alpha = 2^\circ$  with a 0.30c split flap at  $\delta = 45^\circ$ .

This addition has been made for the example cited. In figure 9 the distributions of  $P_{as}$ ,  $P_{bs}$ , and  $P_s$  are given.

The incremental normal-force distribution may be added to the normal-force distribution for the airfoil

with flap neutral (as may be obtained from an experimental pressure-distribution investigation or by the method of reference 1) to give the normal-force distribution for the airfoil with flap deflected

$$P_2 = P_1 + P_3 \quad (14)$$

The incremental flap section normal-force and flap section hinge-moment coefficients are found as the sum of the contributions from the incremental additional and the incremental basic distributions:

$$\left. \begin{aligned} c_{nfs} &= \frac{n_{fs}}{qEc} = \gamma_{as}c_{na\delta} + \gamma_{bs}c_{nb\delta} \\ c_{hfs} &= \frac{h_{fs}}{qE^{\frac{1}{2}}c^2} = \eta_{as}c_{na\delta} + \eta_{bs}c_{nb\delta} \end{aligned} \right\} \quad (15)$$

where  $n_{fs}$  and  $h_{fs}$  are the incremental flap normal force and hinge moment per unit span, respectively. The values of  $\gamma_{as}$  and  $\eta_{as}$  are given in tables IX and X. Values of  $\gamma_{bs}$  and  $\eta_{bs}$  are given in tables VII and VIII.

For the example cited, from tables IX and X

$$\gamma_{as} = 0.12; \eta_{as} = -0.04$$

and by interpolation from tables VII and VIII

$$\gamma_{bs} = 1.79; \eta_{bs} = -0.77$$

so that, using the values of  $c_{na\delta}$  and  $c_{nb\delta}$  already determined,

$$\begin{aligned} c_{nfs} &= 0.12 (0.52) + 1.79 (0.60) = 1.13 \\ c_{hfs} &= -0.04 (0.52) - 0.77 (0.60) = -0.48 \end{aligned}$$

By a similar method, the flap normal-force and hinge-moment coefficients for the airfoil with flap neutral may be determined from

$$c_{nf1} = \gamma_a c_{na} + \gamma_{bc} c_{nb\delta} + \gamma_{bm} c_{nbm} + \gamma_{a.c.} c_{a.c.} \quad (20)$$

$$c_{hf1} = \eta_a c_{na} + \eta_{bc} c_{nb\delta} + \eta_{bm} c_{nbm} + \eta_{a.c.} c_{a.c.} \quad (21)$$

where  $c_{na}$ ,  $c_{nb\delta}$ , and  $c_{nbm}$  are the normal-force coefficients of the additional, camber basic, and moment basic distributions given in reference 1, and  $c_{a.c.}$  is a measure of the magnitude of the aerodynamic-center distribution given in reference 1. These coefficients may be found from equations (16) to (19) in part I. Values of  $\gamma$  and  $\eta$  are given in tables IX and X.

For the example cited, the pressure-distribution classification is given in table II as C12 and

$$\frac{z_c}{c} = 0.018$$

Hence, from equations (16) to (19),

$$\begin{aligned} c_{nbm} &= -6.30(-0.005) = 0.03 \\ c_{nb\delta} &= 18.75(0.018) = 0.34 \\ c_{na} &= 0.34 - 0.34 - 0.03 = -0.03 \\ c_{a.c.} &= -0.03(0.012) = 0.000 \end{aligned}$$

From tables IX and X

$$\begin{aligned} \gamma_a &= 0.12 & \eta_a &= -0.04 \\ \gamma_{bc} &= 0.09 & \eta_{bc} &= -0.03 \\ \gamma_{bm} &= 0.32 & \eta_{bm} &= -0.11 \end{aligned}$$

so that

$$\begin{aligned} c_{nf1} &= (0.12)(-0.03) + (0.09)(0.34) + (0.32)(0.03) = 0.04 \\ c_{hf1} &= (-0.04)(-0.03) + (-0.03)(0.34) + (-0.11)(0.03) \\ &= -0.01 \end{aligned}$$

The flap normal-force and flap hinge-moment coefficients are, by addition,

$$\left. \begin{aligned} c_{nf2} &= c_{nf1} + c_{nfs} \\ c_{hf2} &= c_{hf1} + c_{hfs} \end{aligned} \right\} \quad (22)$$

For the example cited,

$$\begin{aligned} c_{nf2} &= 0.04 + 1.13 = 1.17 \\ c_{hf2} &= -0.01 - 0.48 = -0.49 \end{aligned}$$

#### THE GENERAL PROCEDURE FOR AN AIRFOIL WITH A SERIALY HINGED FLAP

The incremental distribution for an airfoil with a serially hinged plain flap is obtained by determining the incremental distribution for the airfoil with each of the several flaps deflected and then by adding the various distributions.

This superposition method will always be applicable provided that all flaps of the system are unstalled (i. e., no flap is deflected more than  $15^\circ$ ) with the exception of the final (smallest) flap, which may be stalled or unstalled. If, in a combination of a large flap and a small flap (e. g., a tab), the small flap is deflected oppositely to the large flap, experiment has shown that the method is applicable whether either flap is stalled or not.

It is necessary to integrate the normal-force distribution curve to determine the several flap normal-force and hinge-moment coefficients for the airfoil with serially hinged flaps.

LANGLEY MEMORIAL AERONAUTICAL LABORATORY,  
NATIONAL ADVISORY COMMITTEE FOR AERONAUTICS,  
LANGLEY FIELD, VA., April 12, 1933.

## APPENDIX

## THEORETICAL RELATIONSHIPS FOR THE THIN AIRFOIL WITH PLAIN FLAP

The application of thin-airfoil theory to the problem of the airfoil with a plain flap is detailed in the following section.

Designate  $\left(\frac{d\Gamma}{dx}\right)dx$  as the value of the elemental spanwise circulation at any point  $x$  back of the leading edge of the airfoil of chord  $c$  subjected to the stream velocity  $V$ . Glauert has shown that, if a distribution of vorticity along the chord of the airfoil with a plain flap is assumed in the form

$$\left(\frac{d\Gamma}{dx}\right)dx = cV[A_0(1 + \cos \theta) + \sum_1^{\infty} A_n \sin n\theta \sin \theta]d\theta \quad (A-1)$$

where

$$\theta = \cos^{-1}\left(1 - \frac{2x}{c}\right)$$

or

$$x = \frac{c}{2}(1 - \cos \theta) \quad (A-2)$$

then, in order that Kutta's criterion may be satisfied and that the flow across the chord shall be everywhere tangential to the camber line of the airfoil, the coefficients of equation (A-1) must be given by

$$\left. \begin{aligned} A_0 &= \alpha' + \left(\frac{\pi - \theta_0}{\pi}\right)\delta \\ A_1 &= \left(\frac{2 \sin \theta_0}{\pi}\right)\delta \\ &\dots \dots \dots \\ A_n &= \left(\frac{2 \sin n\theta_0}{n\pi}\right)\delta \end{aligned} \right\} \quad (A-3)$$

where  $\alpha'$  is the angle between the direction of stream flow and the unflapped portion of the airfoil,  $\delta$  is the flap angle measured from the unflapped section, and  $\theta_0$  is the value of  $\theta$  at the flap hinge, i. e.,

$$\left. \begin{aligned} \cos \theta_0 &= -(1 - 2E) \\ \sin \theta_0 &= 2\sqrt{E(1 - E)} \end{aligned} \right\} \quad (A-4)$$

where  $E$  is the flap-chord ratio

$$E = \frac{c_f}{c}$$

The pressure difference  $P$  (in terms of the stream dynamic head  $q$ ) at any point  $x$  along the airfoil section is the lift per unit span experienced by the airfoil at that point in terms of  $q$ , or

$$P = \frac{p}{q} = \frac{dL}{q} \quad (A-5)$$

but, from wing theory, the lift of an element of chord per unit span is

$$dL = \rho V \frac{d\Gamma}{dx} dx \quad (A-6)$$

( $\rho$  is the fluid density) and, since by differentiation of equation (A-2)

$$dx = \frac{1}{2}c \sin \theta d\theta$$

then

$$\begin{aligned} P &= \frac{\rho V^2 c}{q} [A_0(1 + \cos \theta) + \sum_1^{\infty} A_n \sin n\theta \sin \theta] \frac{d\theta}{dx} \\ &= 4[A_0\left(\frac{1 + \cos \theta}{\sin \theta}\right) + \sum_1^{\infty} A_n \sin n\theta] \end{aligned} \quad (A-7)$$

Substituting the value of the coefficients (equation (A-3))

$$P = \left[ \frac{4(1 + \cos \theta)}{\sin \theta} \right] \left[ \alpha' + \left(\frac{\pi - \theta_0}{\pi}\right)\delta \right] + \sum_1^{\infty} \frac{8\delta \sin n\theta_0 \sin n\theta}{n\pi}$$

When the flap is neutral ( $\delta = 0$ ), the lift distribution is (using the subscript 1 for the flap-neutral case)

$$P_1 = \left[ \frac{4(1 + \cos \theta)}{\sin \theta} \right] \alpha' \quad (A-8)$$

The incremental lift distribution due to flap deflection is

$$P_s = \left[ \frac{4(1 + \cos \theta)(\pi - \theta_0)}{\pi \sin \theta} \right] + \sum_1^{\infty} \frac{8 \sin n\theta_0 \sin n\theta}{n\pi} \delta \quad (A-9)$$

Perring (reference 12) has shown that, for airfoils with serially hinged flaps, the elemental chordwise distribution of circulation may be expressed by equation (A-1), provided that the coefficients be given by

$$\left. \begin{aligned} A_0 &= \alpha + \frac{\pi - \theta_{01}}{\pi} \delta_1 + \frac{\pi - \theta_{02}}{\pi} \delta_2 + \dots + \frac{\pi - \theta_{0r}}{\pi} \delta_r \\ A_1 &= \frac{2 \sin \theta_{01}}{\pi} \delta_1 + \frac{2 \sin \theta_{02}}{\pi} \delta_2 + \dots + \frac{2 \sin \theta_{0r}}{\pi} \delta_r \\ &\dots \dots \dots \\ A_n &= \frac{2 \sin n\theta_{01}}{n\pi} \delta_1 + \frac{2 \sin n\theta_{02}}{n\pi} \delta_2 + \dots + \frac{2 \sin n\theta_{0r}}{n\pi} \delta_r \end{aligned} \right\} \quad (A-10)$$

where  $\theta_{01}, \theta_{02}, \dots, \theta_{0r}$  and  $\delta_1, \delta_2, \dots, \delta_r$  are the values of  $\theta_0$  and  $\delta$  for each of the  $r$  number of flaps.

Hence, the lift distribution over an airfoil with serially hinged flaps may be expressed by

$$P_s = P_1 + P_{s1} + P_{s2} + P_{s3} + \dots + P_{sr} \quad (A-11)$$

where  $P_1$  denotes the distribution with all flaps neutral (given by equation (A-8)) and  $P_{s1}, P_{s2}, \dots, P_{sr}$  are the incremental distributions due to the individual deflection of flaps 1, 2,  $\dots, r$ , respectively.

A characteristic feature of the thin-airfoil theory is that the incremental distribution due to the deflection of one or more flaps is independent of the original shape of the mean camber line of an airfoil. An airfoil with a curved mean camber line may be considered essentially

as a symmetrical airfoil with an infinite system of serially hinged flaps deflected so as to produce that curvature. It has already been seen that the incremental distribution due to the deflection of any one of a number of serially hinged flaps is independent of the deflections of any of the other flaps.

Thus the incremental lift distribution as given by equation (A-9) is equally applicable to every flapped airfoil of infinitesimal thickness.

Now consider the incremental lift distribution given by equation (A-9) to be the sum of (1) the incremental additional distribution

$$P_{as} = \left[ \frac{4(\pi - \theta_0)(1 + \cos \theta)}{\pi \sin \theta} \right] \delta \quad (\text{A-12})$$

and (2) the incremental basic distribution

$$P_{bs} = \left[ \sum_1^{\infty} \frac{8 \sin n \theta_0 \sin n \theta}{n \pi} \right] \delta \quad (\text{A-13})$$

The general form of the incremental additional distribution, unlike the incremental basic distribution, is not a function of the flap-chord ratio,  $E$ .

Glauert (reference 3) has shown that the incremental lift coefficient (i. e., for  $\alpha' = 0$ ) is given by

$$c_{ls} = 2[(\pi - \theta_0) + \sin \theta_0] \delta \quad (\text{A-14})$$

The incremental additional lift coefficient is given by

$$\begin{aligned} c_{las} &= \frac{L_{as}}{qc} = \frac{1}{qc} \int_0^c P_{as} q dx \\ &= \frac{2(\pi - \theta_0) \delta}{\pi} \int_0^{\pi} (1 + \cos \theta) d\theta \\ &= 2(\pi - \theta_0) \delta \end{aligned} \quad (\text{A-15})$$

and, from equations (A-14) and (A-15)

$$c_{lbs} = 2 \sin \theta_0 \delta \quad (\text{A-16})$$

Substitution of the values of  $c_{las}$  and  $c_{lbs}$  in equations (A-12) and (A-13), gives

$$\frac{P_{as}}{c_{las}} = \frac{2(1 + \cos \theta)}{\pi \sin \theta} \quad (\text{A-17})$$

$$\frac{P_{bs}}{c_{lbs}} = \frac{4}{\pi \sin \theta_0} \sum_1^{\infty} \frac{\sin n \theta_0 \sin n \theta}{n} \quad (\text{A-18})$$

Equation (A-18) may be rewritten as the sum of two series

$$\frac{P_{bs}}{c_{lbs}} = \frac{2}{\pi \sin \theta_0} \left[ \sum_1^{\infty} \frac{\cos n(\theta_0 - \theta)}{n} - \sum_1^{\infty} \frac{\cos n(\theta_0 + \theta)}{n} \right]$$

But

$$\sum_1^{\infty} \frac{\cos nr}{n} = -\log_e 2 - \log_e \sin \frac{r}{2}$$

Hence

$$\frac{P_{bs}}{c_{lbs}} = \frac{2}{\pi \sin \theta_0} \log_e \left[ \frac{\sin \frac{1}{2}(\theta_0 + \theta)}{\sin \frac{1}{2}(\theta_0 - \theta)} \right] \quad (\text{A-19})$$

The moment of the incremental additional lift about the quarter-chord point of the airfoil may be shown to be zero, hence the incremental basic lift is responsible for the entire incremental quarter-chord moment.

#### REFERENCES

1. Jacobs, Eastman N., and Rhode, R. V.: Airfoil Section Characteristics as Applied to the Prediction of Air Forces and Their Distribution on Wings. T. R. No. 631, N. A. C. A., 1938.
2. Glauert, H.: Theoretical Relationships for an Aerofoil with Hinged Flap. R. & M. No. 1095, British A. R. C., 1927.
3. Glauert, H.: The Elements of Aerofoil and Airscrew Theory. Cambridge University Press, 1930.
4. Jacobs, Eastman N., and Pinkerton, Robert M.: Pressure Distribution over a Symmetrical Airfoil Section with Trailing Edge Flap. T. R. No. 360, N. A. C. A., 1930.
5. Wenzinger, Carl J.: Pressure Distribution over an Airfoil Section with a Flap and Tab. T. R. No. 574, N. A. C. A., 1936.
6. Wallace, Rudolf: Investigation of Full-Scale Split Trailing-Edge Wing Flaps with Various Chord and Hinge Locations. T. R. No. 539, N. A. C. A., 1935.
7. Wenzinger, Carl J., and Harris, Thomas A.: Pressure Distribution over a Rectangular Airfoil with a Partial-Span Split Flap. T. R. No. 571, N. A. C. A., 1936.
8. Pinkerton, Robert M., and Greenberg, Harry: Aerodynamic Characteristics of a Large Number of Airfoils tested in the Variable-Density Tunnel. T. R. No. 628, N. A. C. A., 1938.
9. Wenzinger, Carl J.: Wind-Tunnel Investigation of Ordinary and Split Flaps on Airfoils of Different Profile. T. R. No. 554, N. A. C. A., 1936.
10. Abbott, Ira H., and Greenberg, Harry: Tests in the Variable-Density Wind Tunnel of the N. A. C. A. 23012 Airfoil with Plain and Split Flaps. T. R. (to be published).
11. Jacobs, Eastman N., and Pinkerton, Robert M.: Tests in the Variable-Density Wind Tunnel of Related Airfoils Having the Maximum Camber Unusually Far Forward. T. R. No. 537, N. A. C. A., 1935.
12. Perring, W. G. A.: The Theoretical Relationships for an Aerofoil with a Multiply Hinged Flap System. R. & M. No. 1171, British A. R. C., 1928.

TABLE II  
CHARACTERISTICS FOR 22 AIRFOILS

[Class A distribution has not yet been determined]

Station $z/c$	Class B	Class C	Class D	Class E
0	0	0	0	0
.0125	5.93	4.93	4.32	3.87
.025	4.37	4.23	4.02	3.81
.050	3.20	3.22	3.25	3.27
.075	2.63	2.68	2.76	2.81
.100	2.28	2.32	2.39	2.44
.130	1.77	1.85	1.90	1.95
.200	1.40	1.54	1.58	1.62
.300	1.10	1.14	1.16	1.18
.400	.87	.87	.88	.89
.500	.67	.68	.68	.69
.600	.51	.51	.51	.51
.700	.38	.37	.37	.38
.800	.25	.24	.24	.22
.900	.13	.12	.12	.11
.950	.06	.06	.06	.06
1,000	0	0	0	0

Airfoil	Classification PD	$\alpha$ , c. (percent $c$ ahead of $c/4$ )	Camber (percent $c$ 100 $x_{u/c}$ )
Clark Y	C10	1.1	3.9
Clark YM-15	D10	1.1	4.0
Clark YM-18	E10	1.4	4.0
Curtiss C-72	C10	1.0	4.0
Göttingen 357	D10	.7	5.9
Göttingen 398	D10	.4	4.9
N-22	C10	.6	4.3
N. A. C. A. 0006	A10	.7	0
N. A. C. A. 0012	C10	1.3	0
N. A. C. A. 2212	C12	.9	2.0
N. A. C. A. 2409	B10	.7	2.0
N. A. C. A. 2412	C10	1.2	2.0
N. A. C. A. 2415	D10	1.4	2.0
N. A. C. A. 2418	E10	1.1	2.0
N. A. C. A. 4412	C10	.7	4.0
N. A. C. A. 23012	C12	1.3	1.8
N. A. C. A. CYH	C11	.7	3.1
N. A. C. A. -M6	C11	.4	2.4
R. A. F. 15	A10	1.7	2.6
U. S. A. 27	C10	1.8	5.6
U. S. A. 35-A	E10	.8	7.3
U. S. A. 35-B	C10	.5	4.6

### $P_{bd}/c_{max}$ DISTRIBUTION

(a) PLAIN FLAP AT  $\delta = 5^\circ, 10^\circ, \text{ AND } 15^\circ$

(b) PLAIN FLAP AT  $\delta = 20^\circ$

$E \rightarrow$	0.05	0.10	0.15	0.20	0.25	0.30	0.35	0.40	0.45	0.50	0.55	0.60	0.65	0.70		0.05	0.10	0.15	0.20	0.25	0.30	0.35	0.40	0.45	0.50	0.55	0.60	
$\frac{x/c}{1-E}$ (ahead of hinge)	0.05 0.10 0.20 0.30 0.40 0.50 0.60 0.70 0.80 0.90 1.00	0.15 0.22 0.33 0.43 0.54 0.66 0.79 0.97 1.23 1.78	0.18 0.22 0.34 0.44 0.55 0.68 0.82 1.00 1.24 1.74	0.16 0.22 0.34 0.44 0.55 0.68 0.82 1.00 1.24 1.74	0.19 0.24 0.35 0.45 0.56 0.69 0.83 1.01 1.25 1.75	0.17 0.23 0.34 0.44 0.55 0.68 0.82 1.00 1.24 1.75	0.17 0.23 0.34 0.44 0.55 0.68 0.82 1.00 1.24 1.75	0.18 0.23 0.34 0.44 0.55 0.68 0.82 1.00 1.24 1.75	0.19 0.24 0.35 0.45 0.56 0.69 0.83 1.01 1.25 1.75	0.20 0.25 0.36 0.46 0.57 0.70 0.84 1.01 1.25 1.75	0.21 0.26 0.37 0.47 0.58 0.71 0.85 1.02 1.26 1.76	0.22 0.27 0.38 0.48 0.59 0.72 0.86 1.03 1.27 1.77	0.23 0.28 0.39 0.49 0.60 0.73 0.87 1.04 1.28 1.78	0.25 0.30 0.41 0.51 0.62 0.75 0.89 1.06 1.30 1.79	0.27 0.32 0.43 0.53 0.64 0.77 0.91 1.08 1.32 1.80	0.15 0.22 0.33 0.43 0.54 0.67 0.81 0.98 1.22 1.72	0.15 0.22 0.33 0.43 0.54 0.67 0.81 0.98 1.22 1.72	0.16 0.22 0.33 0.43 0.54 0.67 0.81 0.98 1.22 1.72	0.16 0.22 0.33 0.43 0.54 0.67 0.81 0.98 1.22 1.72	0.17 0.23 0.34 0.44 0.55 0.68 0.82 1.00 1.24 1.74	0.17 0.23 0.34 0.44 0.55 0.68 0.82 1.00 1.24 1.74	0.18 0.24 0.35 0.45 0.56 0.69 0.83 1.01 1.25 1.75	0.19 0.24 0.35 0.45 0.56 0.69 0.83 1.01 1.25 1.75	0.20 0.25 0.36 0.46 0.57 0.70 0.84 1.01 1.25 1.75	0.21 0.26 0.37 0.47 0.58 0.71 0.85 1.02 1.26 1.76	0.22 0.27 0.38 0.48 0.59 0.72 0.86 1.03 1.27 1.77	0.23 0.28 0.39 0.49 0.60 0.73 0.87 1.04 1.28 1.78	
$\frac{1-x/c}{E}$ (back of hinge)	0.05 0.10 0.20 0.30 0.40 0.50 0.60 0.70 0.80 0.90 1.00	0.32 0.43 0.54 0.66 0.79 0.97 1.23 1.78 2.28 2.80	0.19 0.22 0.34 0.44 0.55 0.68 0.82 1.00 1.24 1.74	0.16 0.22 0.34 0.44 0.55 0.68 0.82 1.00 1.24 1.74	0.14 0.20 0.31 0.41 0.52 0.65 0.79 0.97 1.23 1.75	0.12 0.18 0.29 0.39 0.50 0.63 0.77 0.95 1.21 1.76	0.11 0.17 0.28 0.38 0.49 0.62 0.76 0.94 1.20 1.76	0.10 0.16 0.27 0.37 0.48 0.61 0.75 0.93 1.19 1.77	0.09 0.15 0.26 0.36 0.47 0.60 0.74 0.92 1.18 1.78	0.08 0.13 0.24 0.34 0.45 0.58 0.72 0.90 1.16 1.80	0.08 0.13 0.24 0.34 0.45 0.58 0.72 0.90 1.16 1.80	0.08 0.13 0.24 0.34 0.45 0.58 0.72 0.90 1.16 1.80	0.07 0.12 0.23 0.33 0.44 0.57 0.71 0.89 1.15 1.81	0.07 0.12 0.23 0.33 0.44 0.57 0.71 0.89 1.15 1.81	0.16 0.22 0.33 0.43 0.54 0.67 0.81 0.98 1.22 1.72	0.15 0.22 0.33 0.43 0.54 0.67 0.81 0.98 1.22 1.72	0.15 0.22 0.33 0.43 0.54 0.67 0.81 0.98 1.22 1.72	0.15 0.22 0.33 0.43 0.54 0.67 0.81 0.98 1.22 1.72	0.16 0.22 0.33 0.43 0.54 0.67 0.81 0.98 1.22 1.72	0.16 0.22 0.33 0.43 0.54 0.67 0.81 0.98 1.22 1.72	0.17 0.23 0.34 0.44 0.55 0.68 0.82 1.00 1.24 1.74	0.17 0.23 0.34 0.44 0.55 0.68 0.82 1.00 1.24 1.74	0.18 0.24 0.35 0.45 0.56 0.69 0.83 1.01 1.25 1.75	0.19 0.24 0.35 0.45 0.56 0.69 0.83 1.01 1.25 1.75	0.20 0.25 0.36 0.46 0.57 0.70 0.84 1.01 1.25 1.75	0.21 0.26 0.37 0.47 0.58 0.71 0.85 1.02 1.26 1.76	0.22 0.27 0.38 0.48 0.59 0.72 0.86 1.03 1.27 1.77	0.23 0.28 0.39 0.49 0.60 0.73 0.87 1.04 1.28 1.78

(c) PLAIN FLAP AT  $\delta = 30^\circ$

(d) PLAIN OR SPLIT FLAP AT  $\delta = 40^\circ$

$E \rightarrow$	0.05	0.10	0.15	0.20	0.25	0.30	0.35	0.40	0.45	0.50		0.05	0.10	0.15	0.20	0.25	0.30	0.35	0.40
$\frac{x/c}{1-E}$ (ahead of hinge)	0.05 0.10 0.20 0.30 0.40 0.50 0.60 0.70 0.80 0.90 1.00	0.15 0.22 0.33 0.43 0.54 0.66 0.79 0.97 1.23 1.78	0.15 0.22 0.34 0.44 0.55 0.68 0.82 1.00 1.24 1.74	0.16 0.22 0.34 0.44 0.55 0.68 0.82 1.00 1.24 1.74	0.16 0.22 0.34 0.44 0.55 0.68 0.82 1.00 1.24 1.74	0.17 0.23 0.34 0.44 0.55 0.68 0.82 1.00 1.24 1.75	0.17 0.23 0.34 0.44 0.55 0.68 0.82 1.00 1.24 1.75	0.18 0.23 0.34 0.44 0.55 0.68 0.82 1.00 1.24 1.75	0.19 0.24 0.35 0.45 0.56 0.69 0.83 1.01 1.25 1.75	0.20 0.25 0.36 0.46 0.57 0.70 0.84 1.01 1.25 1.75	0.21 0.26 0.37 0.47 0.58 0.71 0.85 1.02 1.26 1.76	0.15 0.22 0.33 0.43 0.54 0.67 0.81 0.98 1.22 1.72	0.15 0.22 0.33 0.43 0.54 0.67 0.81 0.98 1.22 1.72	0.16 0.22 0.33 0.43 0.54 0.67 0.81 0.98 1.22 1.72	0.16 0.22 0.33 0.43 0.54 0.67 0.81 0.98 1.22 1.72	0.17 0.23 0.34 0.44 0.55 0.68 0.82 1.00 1.24 1.74	0.17 0.23 0.34 0.44 0.55 0.68 0.82 1.00 1.24 1.74	0.18 0.24 0.35 0.45 0.56 0.69 0.83 1.01 1.25 1.75	0.19 0.24 0.35 0.45 0.56 0.69 0.83 1.01 1.25 1.75
$\frac{1-x/c}{E}$ (back of hinge)	0.05 0.10 0.20 0.30 0.40 0.50 0.60 0.70 0.80 0.90 1.00	0.32 0.43 0.54 0.66 0.79 0.97 1.23 1.78 2.28 2.80	0.19 0.22 0.34 0.44 0.55 0.68 0.82 1.00 1.24 1.74	0.16 0.22 0.34 0.44 0.55 0.68 0.82 1.00 1.24 1.74	0.14 0.20 0.31 0.41 0.52 0.65 0.79 0.97 1.23 1.75	0.12 0.18 0.29 0.39 0.50 0.63 0.77 0.95 1.21 1.76	0.11 0.17 0.28 0.38 0.49 0.62 0.76 0.94 1.20 1.76	0.10 0.16 0.27 0.37 0.48 0.61 0.75 0.93 1.19 1.77	0.09 0.15 0.26 0.36 0.47 0.60 0.74 0.92 1.18 1.78	0.08 0.13 0.24 0.34 0.45 0.58 0.72 0.90 1.16 1.80	0.08 0.13 0.24 0.34 0.45 0.58 0.72 0.90 1.16 1.80	0.16 0.22 0.33 0.43 0.54 0.67 0.81 0.98 1.22 1.72	0.15 0.22 0.33 0.43 0.54 0.67 0.81 0.98 1.22 1.72	0.15 0.22 0.33 0.43 0.54 0.67 0.81 0.98 1.22 1.72	0.16 0.22 0.33 0.43 0.54 0.67 0.81 0.98 1.22 1.72	0.17 0.23 0.34 0.44 0.55 0.68 0.82 1.00 1.24 1.74	0.17 0.23 0.34 0.44 0.55 0.68 0.82 1.00 1.24 1.74	0.18 0.24 0.35 0.45 0.56 0.69 0.83 1.01 1.25 1.75	0.19 0.24 0.35 0.45 0.56 0.69 0.83 1.01 1.25 1.75

### $P_{b2}/c_{n2}$ DISTRIBUTION

(e) PLAIN OR SPLIT FLAP AT $\delta=50^\circ$									(f) PLAIN OR SPLIT FLAP AT $\delta=60^\circ$								
$E \rightarrow$		0.05	0.10	0.15	0.20	0.25	0.30	0.35	0.40	0.05	0.10	0.15	0.20	0.25	0.30	0.35	0.40
$\frac{s/c}{1-E}$ (ahead of hinge)	0.05	0.15	0.18	0.16	0.16	0.17	0.17	0.18	0.19	0.15	0.15	0.16	0.16	0.17	0.17	0.18	0.19
	0.10	0.22	0.23	0.23	0.24	0.25	0.25	0.27	0.27	0.22	0.23	0.23	0.24	0.25	0.25	0.26	0.27
	0.20	0.33	0.34	0.35	0.35	0.36	0.38	0.39	0.40	0.33	0.34	0.35	0.36	0.36	0.38	0.39	0.40
	0.30	0.43	0.44	0.45	0.46	0.47	0.49	0.51	0.52	0.43	0.44	0.45	0.46	0.47	0.49	0.51	0.52
	0.40	0.54	0.55	0.56	0.57	0.58	0.60	0.62	0.64	0.54	0.55	0.56	0.57	0.58	0.60	0.62	0.64
	0.50	0.66	0.66	0.68	0.69	0.71	0.73	0.75	0.77	0.66	0.67	0.68	0.69	0.71	0.73	0.75	0.77
	0.60	0.79	0.80	0.82	0.83	0.85	0.88	0.90	0.93	0.79	0.80	0.82	0.83	0.85	0.88	0.90	0.93
	0.70	0.97	0.98	1.00	1.03	1.05	1.08	1.11	1.14	0.97	0.98	0.99	1.01	1.02	1.05	1.07	1.10
	0.80	1.21	1.22	1.23	1.25	1.26	1.29	1.32	1.35	1.20	1.21	1.22	1.24	1.25	1.28	1.29	1.32
	0.90	1.54	1.55	1.56	1.57	1.57	1.57	1.57	1.57	1.52	1.53	1.54	1.56	1.56	1.53	1.51	1.50
$\frac{1-s/c}{E}$ (back of hinge)	1.00	3.81	2.68	2.27	2.00	1.86	1.77	1.71	1.67	3.84	2.59	2.22	1.97	1.81	1.71	1.63	1.59
	0.90	4.18	2.90	2.45	2.15	1.95	1.81	1.73	1.66	4.04	2.80	2.36	2.06	1.88	1.76	1.68	1.62
	0.80	4.25	3.00	2.50	2.20	1.98	1.82	1.72	1.64	4.16	2.94	2.45	2.16	1.94	1.78	1.68	1.59
	0.70	4.27	3.02	2.48	2.18	1.96	1.81	1.70	1.59	4.27	3.02	2.48	2.18	1.96	1.81	1.70	1.59
	0.60	4.21	2.97	2.43	2.14	1.92	1.77	1.65	1.55	4.27	3.01	2.46	2.17	1.95	1.79	1.67	1.57
	0.50	4.07	2.86	2.36	2.06	1.84	1.69	1.57	1.48	4.18	2.93	2.42	2.11	1.89	1.73	1.62	1.52
	0.40	3.86	2.71	2.24	1.95	1.73	1.59	1.48	1.39	4.01	2.82	2.33	2.02	1.80	1.65	1.54	1.45
	0.30	3.52	2.49	2.04	1.75	1.58	1.44	1.34	1.25	3.71	2.62	2.15	1.86	1.66	1.52	1.41	1.32
	0.20	3.06	2.15	1.76	1.53	1.37	1.25	1.16	1.09	3.27	2.29	1.88	1.63	1.46	1.33	1.24	1.16
	0.10	2.34	1.64	1.33	1.16	1.05	0.96	0.90	0.84	2.51	1.76	1.43	1.25	1.13	1.03	0.96	0.90
0.05	2.02	1.22	1.00	0.87	0.78	0.70	0.65	0.61	2.18	1.31	1.08	0.93	0.84	0.76	0.71	0.66	

(g) SPLIT FLAP AT $\delta=20^\circ$											(h) SPLIT FLAP AT $\delta=30^\circ$										
$E \rightarrow$		0.05	0.10	0.15	0.20	0.25	0.30	0.35	0.40	0.45	0.50	0.05	0.10	0.15	0.20	0.25	0.30	0.35	0.40	0.45	0.50
$\frac{s/c}{1-E}$ (ahead of hinge)	0.05	0.15	0.15	0.16	0.16	0.17	0.17	0.18	0.19	0.20	0.21	0.15	0.15	0.16	0.16	0.17	0.17	0.18	0.19	0.20	0.21
	0.10	0.22	0.23	0.23	0.24	0.25	0.25	0.26	0.27	0.29	0.30	0.22	0.23	0.23	0.24	0.25	0.25	0.26	0.27	0.29	0.30
	0.20	0.33	0.34	0.35	0.35	0.36	0.38	0.39	0.40	0.42	0.44	0.33	0.34	0.35	0.36	0.38	0.39	0.40	0.42	0.44	0.46
	0.30	0.43	0.44	0.45	0.46	0.47	0.49	0.51	0.52	0.55	0.57	0.43	0.44	0.45	0.46	0.47	0.49	0.51	0.52	0.56	0.57
	0.40	0.54	0.55	0.56	0.57	0.58	0.60	0.62	0.64	0.67	0.70	0.54	0.55	0.56	0.57	0.58	0.60	0.62	0.64	0.67	0.70
	0.50	0.66	0.66	0.68	0.69	0.71	0.73	0.75	0.77	0.80	0.84	0.66	0.66	0.68	0.69	0.71	0.73	0.75	0.77	0.80	0.84
	0.60	0.79	0.80	0.82	0.83	0.85	0.88	0.90	0.93	0.97	1.00	0.79	0.80	0.82	0.83	0.85	0.88	0.90	0.93	0.96	1.00
	0.70	0.97	0.98	1.00	1.01	1.03	1.05	1.08	1.11	1.15	1.19	0.97	0.98	1.00	1.01	1.03	1.05	1.08	1.11	1.15	1.19
	0.80	1.23	1.24	1.26	1.27	1.29	1.31	1.34	1.38	1.42	1.46	1.23	1.24	1.26	1.27	1.29	1.31	1.34	1.38	1.42	1.46
	0.90	1.69	1.70	1.71	1.73	1.73	1.73	1.73	1.73	1.74	1.74	1.64	1.65	1.66	1.67	1.68	1.68	1.68	1.69	1.70	1.70
$\frac{1-s/c}{E}$ (back of hinge)	1.00	4.79	3.33	2.79	2.44	2.22	2.08	1.97	1.90	1.86	1.84	4.55	3.15	2.63	2.32	2.14	1.98	1.89	1.83	1.78	1.73
	0.90	4.84	3.36	2.83	2.49	2.26	2.09	1.98	1.90	1.83	1.79	4.60	3.19	2.69	2.36	2.14	1.99	1.88	1.80	1.73	1.68
	0.80	4.65	3.29	2.74	2.40	2.16	1.99	1.87	1.78	1.70	1.63	4.49	3.18	2.65	2.32	2.09	1.92	1.81	1.73	1.64	1.58
	0.70	4.32	3.06	2.51	2.21	1.99	1.84	1.72	1.61	1.54	1.48	4.27	3.02	2.48	2.19	1.97	1.82	1.70	1.60	1.52	1.46
	0.60	3.94	2.77	2.27	2.00	1.80	1.65	1.54	1.45	1.38	1.32	4.02	2.83	2.32	2.04	1.83	1.69	1.57	1.48	1.41	1.35
	0.50	3.51	2.46	2.03	1.77	1.59	1.46	1.36	1.28	1.21	1.16	3.71	2.60	2.14	1.87	1.68	1.54	1.43	1.35	1.28	1.22
	0.40	3.05	2.15	1.77	1.64	1.37	1.26	1.17	1.10	1.04	0.99	3.35	2.36	1.94	1.69	1.51	1.38	1.29	1.21	1.15	1.09
	0.30	2.60	1.83	1.51	1.30	1.16	1.06	0.98	0.92	0.88	0.84	2.95	2.08	1.71	1.48	1.32	1.21	1.12	1.05	1.00	0.95
	0.20	2.13	1.60	1.28	1.06	0.95	0.87	0.81	0.76	0.72	0.68	2.68	1.88	1.54	1.33	1.19	1.09	1.01	0.93	0.90	0.85
	0.10	1.54	1.08	0.88	0.77	0.69	0.63	0.59	0.55	0.52	0.49	1.91	1.34	1.08	0.95	0.86	0.79	0.73	0.68	0.64	0.61
0.05	1.29	0.78	0.64	0.55	0.50	0.45	0.42	0.39	0.37	0.35	1.63	0.98	0.81	0.70	0.63	0.57	0.53	0.49	0.47	0.44	

TABLE IV  
VALUES OF  $G$ 

$\delta$ (deg.) $E$	5, 10, 15	20	30	40	50	60
(a) PLAIN FLAPS						
0	-0.474	-0.476	-0.477	-0.478	-0.479	-0.479
.05	-.448	-.451	-.453	-.455	-.456	-.456
.10	-.423	-.426	-.431	-.434	-.435	-.436
.15	-.397	-.404	-.408	-.411	-.414	-.415
.20	-.372	-.380	-.387	-.392	-.395	-.396
.25	-.347	-.357	-.366	-.372	-.375	-.377
.30	-.320	-.334	-.346	-.352	-.357	-.360
.35	-.294	-.311	-.325	-.332	-.339	-.342
.40	-.268	-.283	-.304			
.45	-.242	-.263	-.283			
.50	-.215	-.242				
.55	-.189	-.220				
.60	-.163					
.65	-.136					
.70						
(b) SPLIT FLAPS						
0		-0.476	-0.477	-0.478	-0.479	-0.479
.05		-.452	-.454	-.455	-.456	-.456
.10		-.430	-.432	-.434	-.435	-.436
.15		-.407	-.409	-.411	-.414	-.415
.20		-.385	-.388	-.392	-.395	-.396
.25		-.363	-.367	-.372	-.375	-.377
.30		-.342	-.347	-.352	-.357	-.360
.35		-.320	-.327	-.333	-.339	-.342
.40		-.299	-.307			
.45		-.278	-.287			
.50						
.55						
.60						
.65						
.70						

TABLE V  
VALUES OF  $\tau_n$ 

$\delta$ (deg.) $E$	10	20	30	40	50	60
(a) PLAIN FLAPS						
0	0	0	0	0	0	0
.05	-.00	-.02	-.05	-.09	-.14	-.21
.10	-.01	-.03	-.07	-.14	-.23	-.34
.15	-.01	-.04	-.09	-.18	-.30	-.47
.20	-.01	-.05	-.11	-.23	-.38	-.59
.25	-.01	-.06	-.14	-.27	-.46	-.72
.30	-.02	-.07	-.16	-.32	-.54	-.85
.35	-.02	-.08	-.19	-.37	-.63	-.98
.40	-.02	-.09	-.21	-.42	-.71	-1.11
.45	-.03	-.11	-.25			
.50	-.03	-.12	-.28			
.55	-.04	-.14				
.60	-.05	-.17				
.65	-.06					
.70	-.07					
(b) SPLIT FLAPS						
0		0	0	0	0	0
.05		-.02	-.05	-.09	-.14	-.21
.10		-.03	-.07	-.14	-.23	-.34
.15		-.04	-.10	-.18	-.30	-.47
.20		-.05	-.12	-.23	-.38	-.59
.25		-.06	-.15	-.27	-.46	-.72
.30		-.07	-.17	-.32	-.54	-.85
.35		-.08	-.20	-.37	-.63	-.98
.40		-.10	-.23	-.42	-.71	-1.11
.45		-.11	-.26			
.50		-.13	-.29			
.55						
.60						
.65						
.70						

TABLE VI  
VALUES OF  $\tau_m$ 

$\delta$ (deg.) $E$	10	20	30	40	50	60
(a) PLAIN FLAPS						
0	1.00	1.00	1.00	1.00	1.00	1.00
.05	1.00	1.01	1.03	1.06	1.10	1.15
.10	1.00	1.02	1.05	1.09	1.15	1.23
.15	1.01	1.02	1.06	1.11	1.18	1.28
.20	1.01	1.03	1.06	1.12	1.21	1.32
.25	1.01	1.03	1.07	1.14	1.23	1.36
.30	1.01	1.03	1.07	1.14	1.24	1.38
.35	1.01	1.03	1.07	1.15	1.25	1.39
.40	1.01	1.03	1.08	1.15	1.25	1.39
.45	1.01	1.03	1.07			
.50	1.01	1.03	1.07			
.55	1.01	1.03				
.60	1.01	1.03				
.65	1.01					
.70	1.00					
(b) SPLIT FLAPS						
0		1.00	1.00	1.00	1.00	1.00
.05		1.01	1.03	1.06	1.10	1.15
.10		1.02	1.05	1.09	1.15	1.23
.15		1.02	1.06	1.11	1.18	1.28
.20		1.03	1.07	1.12	1.21	1.32
.25		1.03	1.07	1.14	1.23	1.36
.30		1.03	1.08	1.14	1.24	1.38
.35		1.03	1.08	1.15	1.25	1.39
.40		1.03	1.08	1.15	1.25	1.39
.45		1.03	1.08			
.50		1.03	1.07			
.55						
.60						
.65						
.70						

TABLE VII  
NORMAL-FORCE PARAMETER  $\gamma_{81}$ 

$\delta$ (deg.) $E$	5, 10, 15	20	30	40	50	60
(a) PLAIN FLAPS						
0.05	2.81	2.97	3.11	3.36	3.47	3.52
.10	2.04	2.15	2.25	2.43	2.51	2.55
.15	1.68	1.78	1.87	2.02	2.08	2.13
.20	1.48	1.56	1.64	1.77	1.82	1.85
.25	1.34	1.41	1.49	1.60	1.64	1.67
.30	1.24	1.30	1.36	1.48	1.52	1.55
.35	1.16	1.22	1.28	1.39	1.43	1.45
.40	1.10	1.16	1.21	1.31	1.35	1.37
.45	1.04	1.10	1.16			
.50	1.00	1.06	1.11			
.55	.97	1.02				
.60	.94	.99				
.65	.91					
.70	.88					
(b) SPLIT FLAPS						
0.05		3.19	3.29	3.36	3.47	3.52
.10		2.31	2.38	2.43	2.51	2.55
.15		1.91	1.97	2.02	2.08	2.13
.20		1.68	1.73	1.77	1.82	1.85
.25		1.52	1.57	1.60	1.64	1.67
.30		1.41	1.45	1.48	1.52	1.55
.35		1.32	1.36	1.39	1.43	1.45
.40		1.25	1.28	1.31	1.35	1.37
.45		1.19	1.22			
.50		1.14	1.17			
.55						
.60						
.65						
.70						

TABLE VIII  
HINGE-MOMENT PARAMETER  $\eta_{hs}$

$\delta$ (deg.) E	5, 10, 15	20	30	40	50	60
(a) PLAIN FLAPS						
0.05	-0.88	-1.23	-1.38	-1.48	-1.59	-1.63
.10	-.61	-.81	-.96	-1.04	-1.12	-1.16
.15	-.50	-.66	-.79	-.86	-.91	-.95
.20	-.43	-.57	-.68	-.75	-.80	-.83
.25	-.39	-.52	-.61	-.67	-.72	-.74
.30	-.36	-.47	-.57	-.62	-.66	-.68
.35	-.33	-.44	-.53	-.57	-.62	-.64
.40	-.32	-.42	-.49	-.54	-.58	-.60
.45	-.30	-.40	-.47			
.50	-.29	-.38	-.45			
.55	-.28	-.36				
.60	-.26	-.35				
.65	-.25					
.70	-.24					
(b) SPLIT FLAPS						
0.05		-1.27	-1.38	-1.48	-1.59	-1.63
.10		-.91	-.99	-1.04	-1.12	-1.16
.15		-.75	-.81	-.86	-.91	-.95
.20		-.64	-.70	-.75	-.80	-.83
.25		-.58	-.63	-.67	-.72	-.74
.30		-.58	-.63	-.67	-.72	-.74
.35		-.50	-.54	-.57	-.62	-.64
.40		-.47	-.51	-.54	-.58	-.60
.45		-.44	-.48			
.50		-.42	-.46			

TABLE IX  
FLAP NORMAL-FORCE PARAMETERS

E	$\gamma_a$ or $\gamma_{as}$	$\gamma_{hs}$ Class 1	$\gamma_{hs}$ Class 2	$\gamma_{hs}$ Class 1	$\gamma_{as}$
0	0	0	0	0	0
.05	-.03	-.13	.02	.09	-4.40
.10	-.06	-.25	.05	.17	-4.95
.15	-.09	-.34	.07	.24	-5.05
.20	-.12	-.40	.09	.32	-4.95
.25	-.15	-.43	.12	.38	-4.78
.30	-.18	-.42	.14	.45	-4.62
.35	-.21	-.37	.17	.51	-4.24
.40	-.25	-.28	.20	.58	-3.93
.45	-.28	-.18	.24	.63	-3.61
.50	-.31	-.01	.28	.69	-3.29
.55	-.35	.14	.32	.74	-2.95
.60	-.39	.30	.38	.79	-2.62
.65	-.43	.45	.43	.84	-2.27
.70	-.47	.60	.47	.89	-1.93

TABLE X.—FLAP HINGE-MOMENT PARAMETERS

E	$\eta_a$ or $\eta_{as}$	$\eta_{hs}$ Class 1	$\eta_{hs}$ Class 2	$\eta_{hs}$ Class 1	$\eta_{as}$
0	0	0	0	0	0
.05	-.01	.04	-.01	-.03	1.05
.10	-.02	.09	-.02	-.06	2.22
.15	-.03	.13	-.02	-.08	2.33
.20	-.04	.10	-.03	-.11	2.37
.25	-.05	.18	-.04	-.13	2.39
.30	-.06	.19	-.05	-.16	2.36
.35	-.07	.19	-.06	-.18	2.31
.40	-.08	.19	-.06	-.20	2.25
.45	-.09	.17	-.07	-.22	2.17
.50	-.10	.14	-.08	-.24	2.09
.55	-.11	.11	-.09	-.26	2.00
.60	-.13	.08	-.11	-.28	1.91
.65	-.14	.04	-.12	-.30	1.81
.70	-.15	.00	-.13	-.32	1.71